Original scientific paper

Informacije MIDEM
Journal of Microelectronics,
Electronic Components and Materials
Vol. 46, No. 3(2016), 154 – 159

Control of electrical conductivity in $0.7BiFeO_3$-$0.3SrTiO_3$ ferroelectric ceramics via thermal treatment in nitrogen atmosphere and Mn doping

Maja Makarovič[1,2], Julian Walker[3], Evgeniya Khomyakova[1,2], Andreja Benčan[1,2], Barbara Malič[1,2] and Tadej Rojac[1,2]

[1]Jožef Stefan Institute, Ljubljana, Slovenia
[2]Jožef Stefan International Postgraduate School, Ljubljana, Slovenia
[3]Materials Research Institute, Pennsylvania State University, USA

Abstract: In this work, the solid solution between polar $BiFeO_3$ (BFO) and non-polar $SrTiO_3$ (ST) with the composition 0.7BFO-0.3ST has been prepared by mechanochemical activation-assisted synthesis with particular emphasis on the characterization and control of the electrical conductivity of the resulting ceramics. According to X-ray diffraction analysis and scanning electron microscopy the incorporation of ST into BFO minimizes the formation of secondary phases, typically formed during the synthesis of unmodified BFO. The as-sintered ceramics exhibited a high electrical conductivity, which was suppressed by post-annealing in N_2 atmosphere. However, this approach showed two major drawbacks: i) re-oxidation of samples and thus increase in their conductivity when annealed in air to elevated temperatures (up to ~450 °C) and ii) increased conductivity by application of high electrical fields, resulting in a strong leakage-current contribution to the measured polarization-electric-field hysteresis loops. For these reasons, in order to reduce the conductivity, we propose here an alternative approach, i.e., doping with MnO_2. Using the doping, the specific conductivity has been decreased and did not deteriorate when the samples were heated in air to elevated temperatures. Unlike in the case of N_2-annealed samples, in the doped samples, saturated ferroelectric loops with negligible leakage-current contributions have been measured, revealing a coercive field of E_c~80 kV/cm and a remanent polarization of $2P_r$~100 μC/cm^2.

Keywords: ferroelectric; $BiFeO_3$-$SrTiO_3$; electrical conductivity

Kontrola električne prevodnosti v feroelektrični keramiki $0.7BiFeO_3$-$0.3SrTiO_3$ z žganjem v dušikovi atmosferi in dopiranjem z Mn

Izvleček: V tem prispevku smo z mehanokemijsko aktivacijo pripravili trdno raztopino med polarnim $BiFeO_3$ (BFO) in nepolarnim $SrTiO_3$ (ST) s sestavo 0.7BFO-0.3ST, pri čemer je bil poseben poudarek na karakterizaciji ter kontroli električne prevodnosti pripravljene keramike. Glede na rezultate rentgenske praškovne difrakcije in vrstične elektronske mikroskopije, vgradnja ST v BFO zmanjša koncentracijo sekundarnih faz v keramiki, ki sicer tipično nastajajo pri sintezi nemodificiranega BFO. Tako pripravljena BFO-ST keramika je pokazala visoko električno prevodnost, ki pa je bila uspešno zmanjšana z naknadnim žganjem pri 750 °C v atmosferi N_2. Kljub temu je ta pristop pokazal dve pomanjkljivosti: i) ponovno oksidacijo ter posledično povečanje električne prevodnosti vzorcev, po tem ko so bili na zraku izpostavljeni povišanim temperaturam (~ 450 °C) ter ii) povečanje prevodnosti pri visokem električnem polju, kar se odraža v velikem prispevku enosmernega električnega toka k izmerjeni histerezni zanki polarizacije v odvisnosti od električnega polja. Zaradi navedenih razlogov, smo se za zmanjševanje prevodnosti odločili za alternativni pristop, tj. dopiranje z MnO_2. Z uporabo tega pristopa je bila specifična prevodnost zmanjšana in se ni spremenila po segrevanju vzorcev na zraku pri povišanih temperaturah. Za razliko od vzorcev žganih v atmosferi N_2, je bil v zankah dopiranih vzorcev razviden zanemarljiv prispevek prevodnosti materiala; vrednost koercitivnega polja je bila E_c ~80 kV/cm, remanentne polarizacije pa $2P_r$ ~100 μC/cm^2.

Ključne besede: feroelektrik; $BiFeO_3$-$SrTiO_3$; električna prevodnost

** Corresponding Author's e-mail: maja.makarovic@ijs.si*

1 Introduction

Bismuth ferrite, $BiFeO_3$ (BFO), is of interest due to its ferroelectric and antiferromagnetic properties at room temperature and due to its high Curie temperature (~820 °C), which make BFO a prime candidate for high-temperature piezoelectric applications [1]. The practical use of BFO has, however, been limited by several factors, including: i) the difficulty to prepare single-phase BFO in bulk form without the presence of secondary phases, which is related to the thermodynamic phase instability of BFO at the temperature range of ceramics processing, ii) the high electrical conductivity due to the mixed valence state $Fe^{4+}/Fe^{3+}/Fe^{2+}$ and iii) the high coercive field for ferroelectric domain switching [2]. One method to suppress the formation of secondary phases, improve the electrical insulation and maintain a relatively high Curie temperature is the incorporation of other ABO_3 perovskites, such as $PbTiO_3$ (PT)[3], $CaTiO_3$ (CT)[4], $BaTiO_3$ (BT)[5] and $SrTiO_3$ (ST)[6], in solid solutions with BFO. Pseudo-binary BFO-ABO_3 solid solution systems between BFO and other perovskites is also of great interest because of the possibility of inducing a morphotropic phase boundary (MPB) where piezoelectric properties are enhanced [7].

It has been shown in several cases that BFO-based solid solutions still exhibit high electrical conductivity. As a result, additional methods to improve the electrical insulation are required. In BFO, which is a p-type conductor, one such method is the annealing of the ceramics in an inert atmosphere with low partial pressure of oxygen, e.g., N_2 [8]. Another method is chemical doping with, e.g., La, Ga, Ti and Mn [5, 9–11]. In particular, Mn doping has been shown to be highly effective in improving the electrical resistivity of BFO-BT ceramics.

Among the BFO-based solid solutions, the solid solution between polar BFO and non-polar ST has been less investigated with little literature data regarding its electrical and electromechanical properties [6, 12, 13]. The dielectric and magnetic properties of this system as well as the potential to exhibit an MPB between a polar and non-polar phase, for which a large piezoelectric response has recently been predicted [14], make this solid solution system particularly interesting.

The aim of this work was to prepare a BFO-ST solid solution in the rhombohedral (ferroelectric) region of the phase diagram reported by Fedulov [6] with the composition containing 70 mol% of BFO (0.7BFO-0.3ST), and to measure the dielectric and ferroelectric properties. Dense ceramics with minimum amount of inhomogeneities were prepared by an alternative processing method, i.e., mechanochemical activation-assisted synthesis. In particular, the effect of post-annealing in nitrogen and Mn doping on the electrical conductivity was investigated.

2 Experimental work

2.1 Synthesis of the solid solution

The solid solution with the composition $0.7BiFeO_3$-$0.3SrTiO_3$ (0.7BFO-0.3STO) was prepared by mechanochemical activation-assisted synthesis using Bi_2O_3 (99.999%, Alfa Aesar), Fe_2O_3 (99.998%, Alfa Aesar), TiO_2 (99.8%, Alfa Aesar) and $SrCO_3$ (99.994% Alfa Aesar) as starting powders. After being separately milled in an absolute ethanol, the powders were weighed according to the stoichiometric ratio in a 35 g mixture and homogenized in a planetary mill (Retsch PM 400, Retsch, Haan, Germany) at 200 min^{-1} for 4 h in absolute ethanol. The mixture was then dried and high-energy milled in a Fritch Pulverisette 7 Vario-Mill (Fritsch GmbH, Idar-Oberstein, Germany) for 40 h in an 80-ml tungsten carbide vial, filled with 14 tungsten carbide milling balls with diameters of 10 mm. The disk rotational frequency and the vial-to-disk rotational frequency were set to, respectively, 300 min^{-1} and -2 (the negative sign denotes the opposite directions of the rotations of the vial and the disk). After the high-energy milling, the mixture was re-milled in a planetary mill in an absolute ethanol at 200 min^{-1} for 4 h. Finally, the powder was dried, pressed into pellets with 150 MPa of uniaxial pressure and sintered in air at 1025 °C for 2 h using a heating/cooling rate of 5 °C/min.

2.2 Post-annealing in N_2

In order to reduce the electrical conductivity of the samples, the sintered samples were post-annealed in N_2 atmosphere. The samples were annealed in a nitrogen gas flow (N_2 4.6, Messer) at 750 °C for 1 h with a heating/cooling rate of 2 °C/min.

2.3 Mn doping

0.1 wt% of pre-milled MnO_2 (99.9%, Alfa Aesar) was added to the activated (high-energy milled) powder. The mixture was homogenized in a planetary mill with absolute ethanol at 200 min^{-1} for 4 h. The powders were then pressed into pellets and sintered in air at 1025 °C for 2 h using a heating/cooling rate of 5 °C/min.

2.4 Characterization of the sintered ceramics

The relative geometric density of sintered ceramics was determined using the theoretical density of 0.7BFO-0.3ST solid solution (7.40 g/cm). This theoretical den-

sity was evaluated based on the theoretical density of individual perovskites, i.e., BFO (8.34 g/cm) and ST (5.12 g/cm), and their volume proportion in the solid solution.

The phase composition of sintered ceramics was determined using X-ray powder diffraction (XRD) analysis (PANalytical X'Pert PRO diffractometer with CuKα$_1$ radiation). The XRD patterns were recorded in a 2θ-range from 20° to 78° with a step of 0.016° and an acquisition time of 100 s. The microstructure of sintered ceramics was examined by field emission scanning electron microscope (FE-SEM, JSM-7600F, Jeol) equipped with a LINK ISIS 300 (Oxford Instruments, Abingdon, U.K.) energy dispersive X-ray spectrometer (EDXS).

For characterization of electrical properties, the sintered pellets were thinned to ~0.2 mm, polished and electroded with Au by sputtering. The dielectric permittivity and loss tangent as a function frequency were analyzed in the range 10^6-10^{-2} Hz using a HP4284A impedance analyzer (frequency range 10^6-10^2 Hz) and Kistler charge amplifier (frequency range 10^3-10^{-2} Hz). High-electric-field polarization and strain hysteresis loops were measured by applying to the samples single sinusoidal electric-field waveforms using an aixACCT TF 2000 analyzer equipped with a laser interferometer.

3 Results and discussion

3.1 Phase composition

Figure 1 shows the XRD patterns of 0.7BFO-0.3ST solid solution along with the end members of the solid solution (BFO and ST) for reference. The XRD pattern of 0.7BFO-0.3ST confirms the presence of the perovskite phase with no detectable secondary phases. By close inspection of the peaks of BFO and ST belonging to the $\{111\}_{pc}$ (pc denotes pseudo cubic notation) family of crystallographic planes (Figure 1 inset), it can be observed that BFO exhibits a pronounced $\{111\}_{pc}$ splitting to $(111)_{pc}$ and $(11\bar{1})_{pc}$ peaks due to the rhombohedral unit-cell distortion, while ST exhibits a single (111) peak because of its cubic structure. Relative to BFO, BFO-ST exhibit a much weaker $\{111\}_{pc}$ peak splitting, indicating that the structure is probably still rhombohedral but with a decreased lattice distortion (rhombohedral angle closer to 90°, where 90° corresponds to cubic lattice)

With respect to BFO, all perovskite peaks of BFO-ST are shifted towards higher 2θ angles, indicating a contraction in unit cell volume by the addition of ST to BFO.

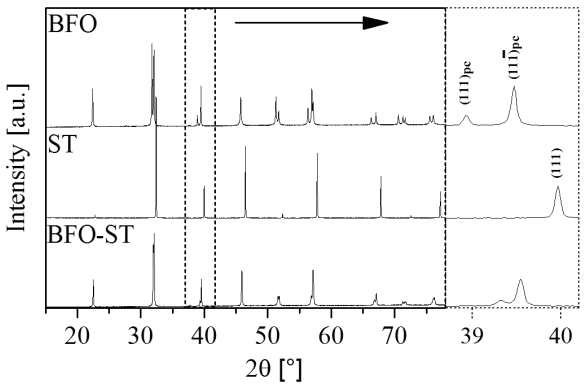

Figure 1: XRD patterns of BFO, ST and 0.7BFO-0.3ST solid solution. The inset on the right side of the figure shows an enlarged view of the peaks belonging to the $\{111\}_{pc}$ family of crystallographic planes.

3.2 Microstructure

The microstructure and phase composition of the sintered ceramics were investigated by FE-SEM (Figure 2). The ceramics exhibit a dense microstructure, consistent with the measured relative density (ρ_{rel}) of ~97%. The chemical homogeneity of the rhombohedral perovskite matrix phase was investigated using EDXS analysis performed on 14 randomly selected points. The standard deviations calculated over all measurements for Bi, Fe, Sr and Ti were 0.7, 1.2, 1.9 and 2.1 %, respectively. The uncertainty of a standard-less EDS analysis was reported to be ±5% relative [15]. These results show that the deviations within the analyzed sample are smaller than the uncertainty of the method, indicating the homogeneous distribution of the elements. However, a closer inspection of the microstructure (see the inset in Figure 2) revealed small, submicron sized

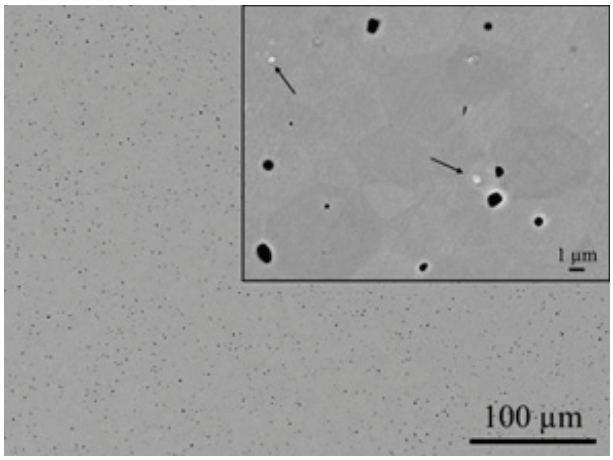

Figure 2: Backscattered electron SEM micrograph of sintered 0.7BFO-0.3ST ceramics. The inset on the right side shows inhomogeneities (marked with arrows).

chemically inhomogeneous inclusions, the concentration of which is evidently insufficient to be detected by XRD, since the ceramics was identified as single phase using XRD analysis (Figure 1).

3.3 Dielectric properties

The real part of the complex dielectric permittivity (ε'), the dielectric loss tangent (*tanδ*) and the real part of the complex electrical conductivity (σ') were studied as a function of frequency for the 0.7BFO-0.3ST ceramics. The real part of the electrical conductivity σ' for each frequency data point was calculated from the measured imaginary dielectric permittivity (ε_d'') and frequency ω using equation (1):

$$\sigma' = \omega\varepsilon_0\varepsilon_d'' \quad (1)$$

where ε_0 is the permittivity of vacuum.

Four different samples have been analyzed: i) as-sintered (undoped) ceramics (□), which was ii) post-annealed in N_2 at 750 °C (○), and iii) additionally annealed in air at ~450 °C after the N_2 annealing (●) and iv) Mn-doped ceramics (▽).

The as-sintered ceramics (Fig. 3, □) exhibit two relaxations in the measured frequency range, observed as two step-like features in ε' within the frequency range 10^1-10^5 Hz, which are accompanied by two peaks in *tanδ*. These relaxations result in high apparent ε' values at the low frequency limit (ε'>10^5 below 10^{-2} Hz). Such relaxation behavior in BFO has been earlier attributed to either Maxwell Wagner-like or polaron hopping conduction mechanisms [2], both in principle related to the elevated electrical conductivity of the ceramics.

After the sintered 0.7BFO-0.3STceramics were annealed in N_2, the dielectric relaxations were largely suppressed (Fig. 3, ○). From the frequency dependent σ', it is possible to estimate the specific electrical conductivity (σ_0) using further expansion of equation 1 into equation 2:

$$\sigma' = \sigma_0 + \omega\varepsilon_0\varepsilon_d'' \quad (2)$$

where ε_d'' is the imaginary part of the dielectric permittivity related to dielectric (or polarization) losses. At low frequencies, if the term $\omega\varepsilon_0\varepsilon_d''$ is sufficiently small, σ' in principle reaches a plateau and σ_0 can be estimated as $\sigma' \approx \sigma_0$. Even though this plateau in σ' has not been reached in the as-sintered (Fig. 3c, □) and N_2-annealed (Fig. 3c, ○) samples, the lower values of σ' of the last-mentioned sample in the low-frequency range indicate a reduction of the electrical conductivity, possibly related to the reduction of Fe^{4+} to Fe^{3+} ions during N_2-annealing as earlier reported for BFO. [8] However, after the same sample was annealed at ~450˚C in air, the dielectric relaxation was again observed. Therefore, the results suggest that the sample re-oxidizes during annealing in air, meaning that the annealing in N_2 has limited practical implications in reducing efficiently the electrical conductivity of BFO-ST.

Similar as in the case of N_2-annealing, Mn doping suppressed the dielectric relaxation originally observed in the as-sintered and undoped sample, resulting in a similar ε', *tanδ* and σ'. In a strong contrast, however, the electrical conductivity and the associated relaxation of this doped composition did not deteriorate after the sample was heated in air at ~450˚C (not shown).

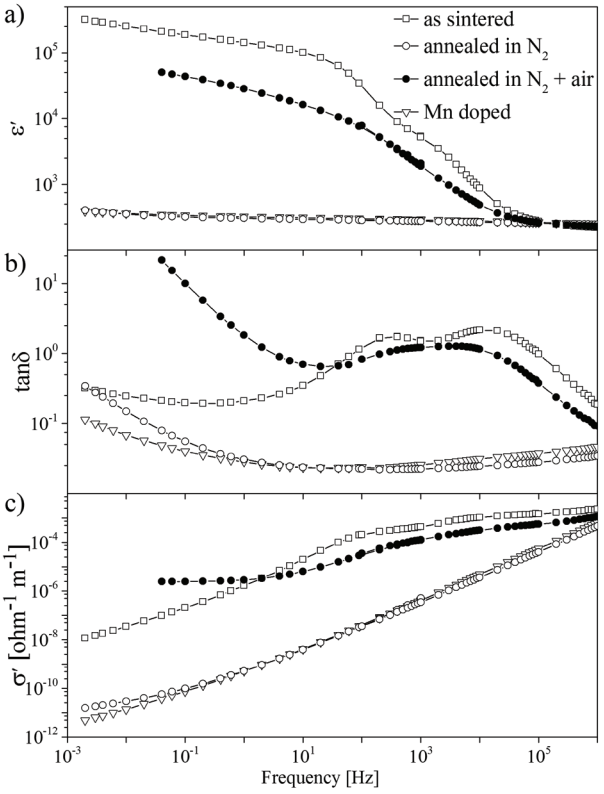

Figure 3: a) Room-temperature real part of complex dielectric permittivity (ε'), b) dielectric loss tangent (*tanδ*) and c) real part of complex electrical conductivity (σ') as a function of frequency for 0.7BFO-0.3ST as-sintered ceramics (□), annealed in N_2 at 750 °C (○) and additionally annealed in air at 450°C (●), and doped with MnO_2 (▽).

3.4 Ferroelectric properties

The polarization-electric-field (P-E) hysteresis loops of 0.7BFO-0.3ST ceramics annealed in N_2 and doped with Mn are shown in Figure 4. The loops were measured at room temperature at 120 kV/cm and frequency of 100 Hz and 10 Hz for the annealed and the doped sample, respectively. The test frequencies were different be-

cause the N_2-annealed ceramics experienced high leakage currents and dielectric breakdown at test frequencies below 100 Hz. Despite the difference in the test frequency, the comparison of the loops can still be used to achieve a qualitative assessment of the different high electric-field behavior of each ceramic. The P-E loop of the N_2-annealed sample is not saturated and shows high leakage-current contribution, evidenced by the rounded shape of the loop. On the contrary, the P-E loop of Mn-doped sample shows approximately saturated loops, signified by the sharp corners at the maximum and minimum electric fields, with the coercive field E_c ~80 kV/cm and remanent polarization $2P_r$ ~100 μC/cm^2. The inset on the right side of the figure shows the loops for the corresponding samples at 10 kV/cm. By comparing the loops of the N_2 annealed sample at 10 kV/cm and 120 kV/cm it can be observed, that there is an abrupt increase in conductivity at high electrical fields, which results in strong leakage-current contribution to the measured polarization-electric-field loops (rounded loop in Fig. 4).

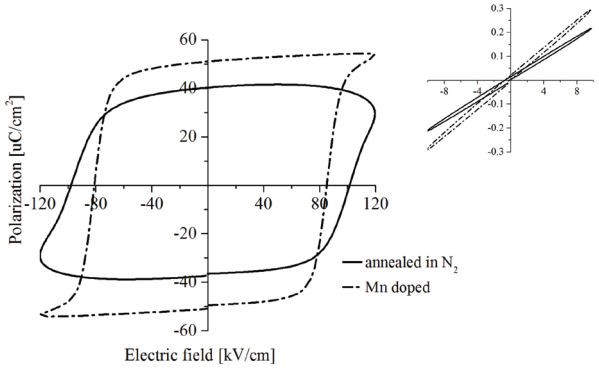

Figure 4: Room temperature P-E loops of 0.7BFO-0.3ST ceramics annealed in N_2 and Mn doped measured at 120 kV/cm. The inset on the right side shows P-E loops of the same samples measured at 10 kV/cm.

4 Conclusions

In the present report, ceramics with composition 0.7BFO-0.3ST were prepared by mechanochemical activation-assisted synthesis, with high chemical homogeneity and high bulk density. The as-sintered samples exhibited high electrical conductivity, which was successfully suppressed by i) post-annealing of the sintered samples in a nitrogen flow or ii) doping with Mn. However, the exposure of the annealed samples to elevated temperature in air resulted in re-oxidation of the samples and consequently re-gain of the high electrical conductivity. In addition, the P-E loops of post-annealed samples showed increased conductivity at high electrical fields, resulting in leakage-current dominated P-E loops. In contrast to the post-annealing in N_2 atmosphere, the doping with Mn has been proven as an efficient method to reduce the electrical conductivity in this system. As expected, the conductivity of Mn-doped samples did not deteriorate when heated in air to elevated temperatures. The P-E loops were saturated with E_c ~80 kV/cm and $2P_r$ ~100μC/cm^2.

5 Acknowledgments

This work was supported by the Slovenian Research Agency (program P2-0105 and project J2-5483).

6 References

1. G. Catalan and J. F. Scott, "Physics and Applications of Bismuth Ferrite," *Adv. Mater.*, vol. 21, no. 24, pp. 2463–2485, Jun. 2009.
2. T. Rojac, A. Bencan, B. Malic, G. Tutuncu, J. L. Jones, J. E. Daniels, and D. Damjanovic, "$BiFeO_3$ Ceramics: Processing, Electrical, and Electromechanical Properties," *J. Am. Ceram. Soc.*, vol. 97, no. 7, pp. 1993–2011, Jul. 2014.
3. T. P. Comyn, S. P. McBride, and a. J. Bell, "Processing and electrical properties of $BiFeO_3$–$PbTiO_3$ ceramics," *Mater. Lett.*, vol. 58, pp. 3844–3846, 2004.
4. Q. Q. Wang, Z. Wang, X. Q. Liu, and X. M. Chen, "Improved Structure Stability and Multiferroic Characteristics in $CaTiO_3$-Modified $BiFeO_3$ Ceramics," *J. Am. Ceram. Soc.*, vol. 95, pp. 670–675, 2012.
5 S. O. Leontsev and R. E. Eitel, "Dielectric and Piezo. electric Properties in Mn-Modified (1-x)$BiFeO_3$-x$BaTiO_3$ Ceramics," *J. Am. Ceram. Soc.*, vol. 92, no. 25823, pp. 2957–2961, 2009.
6. Y. N. Fedulov, S.A., Pyatigorskaya, I., Venevtsev, "An investigation of the $BiFeO_3$-$SrTiO_3$ system," *Sov. Phys. - Crystallogr.*, vol. 10, no. 3, pp. 291–296, 1965.
7. H. Jaffe, B., Cook, W.R.J., Jaffe, *Piezoelectric Ceramics*, US. New York: Academic Press, 1971, p. 316.
8. N. Masó and A. R. West, "Electrical Properties of Ca-Doped $BiFeO_3$ Ceramics: From p -Type Semiconduction to Oxide-Ion Conduction," *Chem. Mater.*, vol. 24, pp. 2127–2132, 2012.
9. J. R. Cheng, R. Eitel, and L. E. Cross, "Lanthanum-modified (1-x)$(Bi_{0.8}La_{0.2})(Ga_{0.05}Fe_{0.95})O_3$-x$PbTiO_3$," *J. Am. Ceram. Soc.*, vol. 86, no. 12, pp. 2111–2115, 2003.
10. K. Kalantari, I. Sterianou, S. Karimi, M. C. Ferrarelli, S. Miao, D. C. Sinclair, and I. M. Reaney, "Ti-Doping to Reduce Conductivity in $Bi_{0.85}Nd_{0.15}FeO_3$ Ceramics," *Adv. Funct. Mater.*, vol. 21, pp. 3737–3743, 2011.

11. H. Yang, C. Zhou, X. Liu, Q. Zhou, G. Chen, H. Wang, and W. Li, "Structural, microstructural and electrical properties of $BiFeO_3$–$BaTiO_3$ ceramics with high thermal stability," *Mater. Res. Bull.*, vol. 47, no. 12, pp. 4233–4239, 2012.
12. S. Vura, P. S. Anil Kumar, A. Senyshyn, and R. Ranjan, "Magneto-structural study of the multiferroic $BiFeO_3$–$SrTiO_3$," *J. Magn. Magn. Mater.*, vol. 365, pp. 76–82, 2014.
13. Z. Z. Ma, Z. M. Tian, J. Q. Li, C. H. Wang, S. X. Huo, H. N. Duan, and S. L. Yuan, "Enhanced polarization and magnetization in multiferroic (1-x) $BiFeO_3$-x$SrTiO_3$ solid solution," *Solid State Sci.*, vol. 13, no. 12, pp. 2196–2200, Dec. 2011.
14. D. Damjanovic, "A morphotropic phase boundary system based on polarization rotation and polarization extension," *Appl. Phys. Lett.*, vol. 97, no. 6, p. 062906, 2010.
15. J. Goldstein, D. Newbury, D. Joy, C. Lyman, P. Echlin, E. Lifshin, L. Sawyer, and J. Michael, *Scanning Electron Microscopy and X-Ray Microanalysis*, Third. New York: KluwerAcademic/Plenum Publisher, 2003.

Arrived: 31. 08. 2016
Accepted: 22. 09. 2016